Cell Reports, Volume *42*

Supplemental information

Progressive development of melanoma-induced cachexia differentially impacts organ systems in mice

Flavia A. Graca, Anna Stephan, Yong-Dong Wang, Abbas Shirinifard, Jianqin Jiao, Peter Vogel, Myriam Labelle, and Fabio Demontis

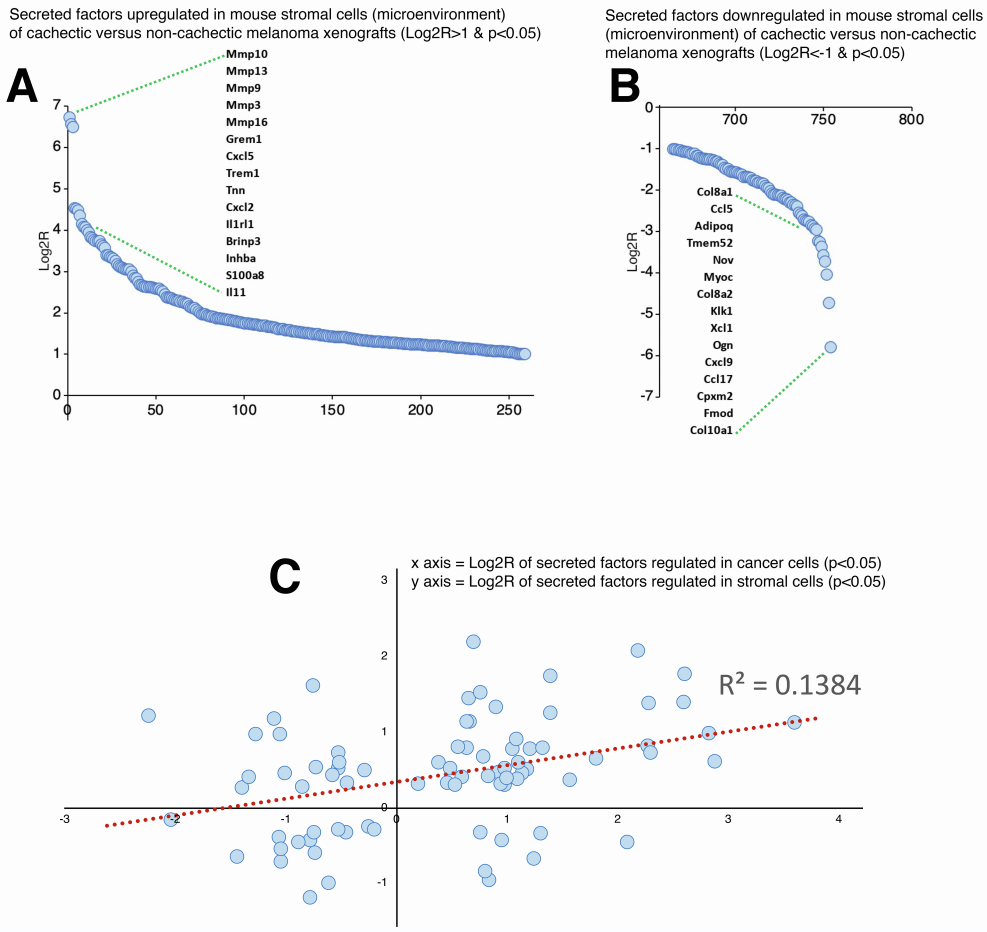

Supplemental Figure S1, Related to Figure 1. The secretome of the mouse stroma is influenced by but differs from that of adjacent human cancer cells. Analysis of the transcriptional changes induced in the mouse stroma (microenvironment) by human cachectic versus non-cachectic melanoma xenografts. Compared to secreted factors expressed by human cachectic melanomas (Fig. 1), the mouse stroma expresses a largely different panel of secreted factors that are upregulated (A) and downregulated (B) by vicinity to cachectic melanoma cells compared to non-cachectic melanoma cells. (C) Analysis of the overall similarity between secreted factors significantly expressed in the cachectic versus non-cachectic cancer cells (x axis) and stroma (y axis) indicates minimal overlap (R^2=0.1384). In (A-B), secreted factors with p<0.05 and Log2R>1 (A) and Log2R<-1 (B) are shown. For comparison in (C), secreted factors with p<0.05 in both conditions are shown, irrespective of the Log2R values.

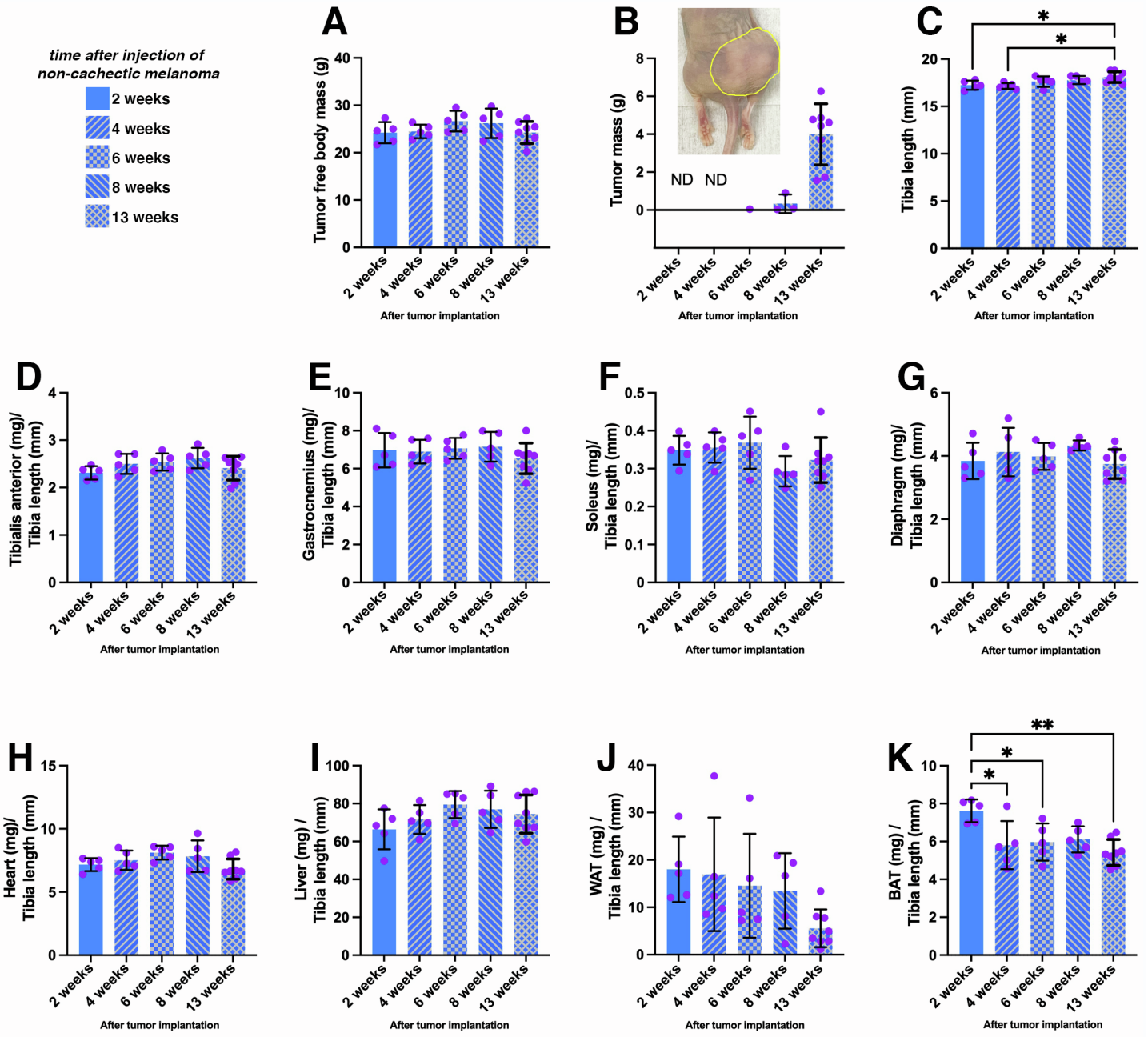

Supplemental Figure S2, Related to Figure 2. The cachexia-non-inducing ("non-cachectic") melanoma tumors do not induce body and tissue wasting. (A) Analysis of mice injected with cachexia-non-inducing ("non-cachectic") melanoma cells. After 13 weeks from cancer cell injection, there is no decline in the tumor-free body mass, even if the tumor mass has reached a substantial size (~4g) at that stage (B). (C) There is a minor but significant increase in the length of the tibia bone from 2 to 13 weeks post cancer cell injection. (D-G) The weight of several skeletal muscles (tibialis anterior, gastrocnemius, soleus, diaphragm) remains unchanged even after 13 weeks from cancer cell injection. (H-J) Likewise, the weight of the heart (H) and liver (I) does not change, whereas (J) there is a trend towards a decline in the weight of the white adipose tissue (WAT). (K) The weight of the brown adipose tissue (BAT) declines from 2 to 4 weeks post cancer cell injection but then remains substantially stable. The graphs report the mean ±SD, the n is indicated; *p<0.05 and **p<0.01.

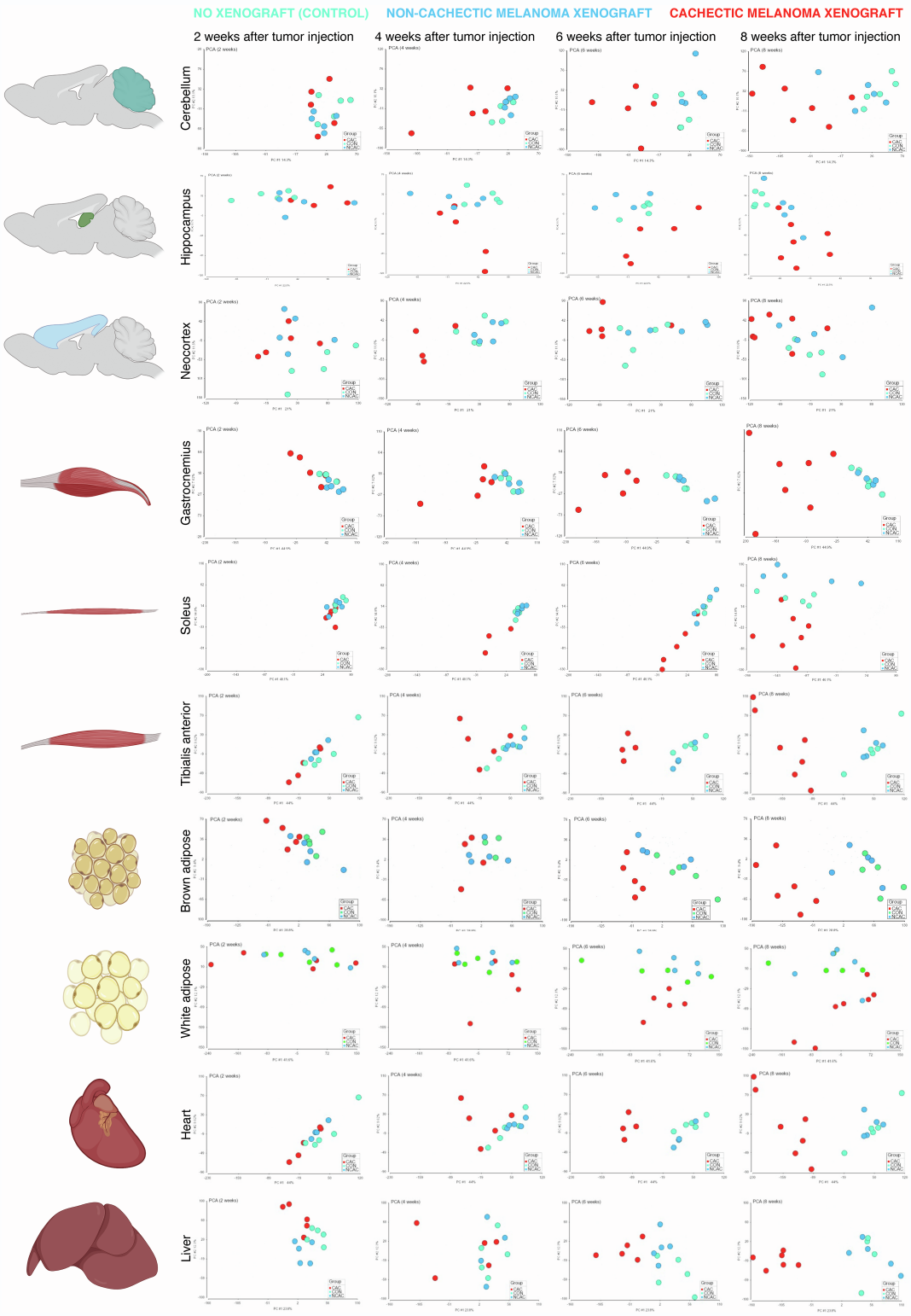

Supplemental Figure S3, Related to Figure 4. Principal Component Analysis (PCA) of RNA-seq from distinct tissues at different time points from implantation of cachexia-inducing ("cachectic") and cachexia-non-inducing ("non-cachectic") melanoma xenografts. Principal Component Analysis (PCA) of RNA-seq data from: brain regions, i.e. cerebellum, hippocampus, and neocortex; skeletal muscles, i.e. gastrocnemius, soleus, and tibialis anterior; brown and white adipose tissues; heart; and liver. PCA indicates that RNA-seq is reproducible because samples of the same group cluster together. Moreover, although cachectic samples co-cluster with control mock-injected and non-cachectic samples at an early time point (2 weeks from tumor implantation), they progressively diverge from control samples at later time points.

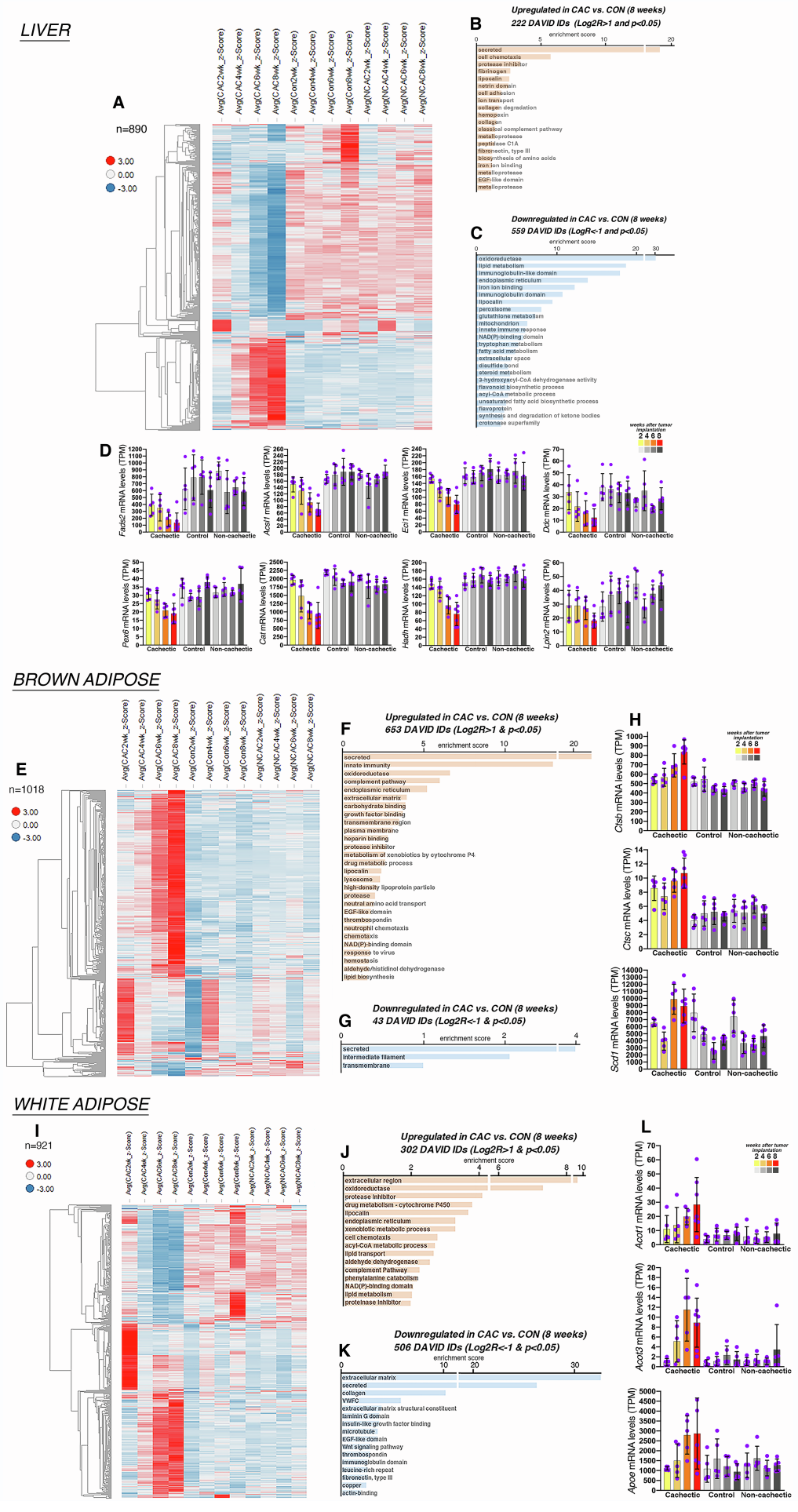
LIVER
A
n=890
3.00
0.00
-3.00
Avg(CAC2wk_z-Score)
Avg(CAC4wk_z-Score)
Avg(CAC6wk_z-Score)
Avg(CAC8wk_z-Score)
Avg(Con2wk_z-Score)
Avg(Con4wk_z-Score)
Avg(Con6wk_z-Score)
Avg(Con8wk_z-Score)
Avg(NCAC2wk_z-Score)
Avg(NCAC4wk_z-Score)
Avg(NCAC6wk_z-Score)
Avg(NCAC8wk_z-Score)
B
Upregulated in CAC vs. CON (8 weeks)
222 DAVID IDs (Log2R>1 and p<0.05)
enrichment score
secreted
cell chemotaxis
protease inhibitor
fibrinogen
lipocalin
netrin domain
cell adhesion
ion transport
collagen degradation
hemopexin
collagen
classical complement pathway
metalloprotease
peptidase C1A
fibronectin, type III
biosynthesis of amino acids
iron ion binding
metalloprotease
EGF-like domain
metalloprotease
C
Downregulated in CAC vs. CON (8 weeks)
559 DAVID IDs (LogR<-1 and p<0.05)
enrichment score
oxidoreductase
lipid metabolism
immunoglobulin-like domain
endoplasmic reticulum
iron ion binding
immunoglobulin domain
lipocalin
peroxisome
glutathione metabolism
mitochondrion
innate immune response
NAD(P)-binding domain
tryptophan metabolism
fatty acid metabolism
extracellular space
disulfide bond
steroid metabolism
3-hydroxyacyl-CoA dehydrogenase activity
flavonoid biosynthetic process
acyl-CoA metabolic process
unsaturated fatty acid biosynthetic process
flavoprotein
synthesis and degradation of ketone bodies
crotonase superfamily
D
weeks after tumor implantation
2 4 6 8
Fads2 mRNA levels (TPM)
Acsl1 mRNA levels (TPM)
Ecl1 mRNA levels (TPM)
Ddc mRNA levels (TPM)
Pex6 mRNA levels (TPM)
Cat mRNA levels (TPM)
Hadh mRNA levels (TPM)
Lpin2 mRNA levels (TPM)
Cachectic
Control
Non-cachectic
BROWN ADIPOSE
E
n=1018
3.00
0.00
-3.00
Avg(CAC2wk_z-Score)
Avg(CAC4wk_z-Score)
Avg(CAC6wk_z-Score)
Avg(CAC8wk_z-Score)
Avg(Con2wk_z-Score)
Avg(Con4wk_z-Score)
Avg(Con6wk_z-Score)
Avg(Con8wk_z-Score)
Avg(NCAC2wk_z-Score)
Avg(NCAC4wk_z-Score)
Avg(NCAC6wk_z-Score)
Avg(NCAC8wk_z-Score)
F
Upregulated in CAC vs. CON (8 weeks)
653 DAVID IDs (Log2R>1 & p<0.05)
enrichment score
secreted
innate immunity
oxidoreductase
complement pathway
endoplasmic reticulum
extracellular matrix
carbohydrate binding
growth factor binding
transmembrane region
plasma membrane
heparin binding
protease inhibitor
metabolism of xenobiotics by cytochrome P4
drug metabolic process
lipocalin
lysosome
high-density lipoprotein particle
protease
neutral amino acid transport
EGF-like domain
thrombospondin
neutrophil chemotaxis
chemotaxis
NAD(P)-binding domain
response to virus
hemostasis
aldehyde/histidinol dehydrogenase
lipid biosynthesis
G
Downregulated in CAC vs. CON (8 weeks)
43 DAVID IDs (Log2R<-1 & p<0.05)
enrichment score
secreted
intermediate filament
transmembrane
H
weeks after tumor implantation
2 4 6 8
Ctsb mRNA levels (TPM)
Ctsc mRNA levels (TPM)
Scd1 mRNA levels (TPM)
Cachectic
Control
Non-cachectic
WHITE ADIPOSE
I
n=921
3.00
0.00
-3.00
Avg(CAC2wk_z-Score)
Avg(CAC4wk_z-Score)
Avg(CAC6wk_z-Score)
Avg(CAC8wk_z-Score)
Avg(Con2wk_z-Score)
Avg(Con4wk_z-Score)
Avg(Con6wk_z-Score)
Avg(Con8wk_z-Score)
Avg(NCAC2wk_z-Score)
Avg(NCAC4wk_z-Score)
Avg(NCAC6wk_z-Score)
Avg(NCAC8wk_z-Score)
J
Upregulated in CAC vs. CON (8 weeks)
302 DAVID IDs (Log2R>1 & p<0.05)
enrichment score
extracellular region
oxidoreductase
protease inhibitor
drug metabolism - cytochrome P450
lipocalin
endoplasmic reticulum
xenobiotic metabolic process
cell chemotaxis
acyl-CoA metabolic process
lipid transport
aldehyde dehydrogenase
complement Pathway
phenylalanine catabolism
NAD(P)-binding domain
lipid metabolism
proteinase inhibitor
K
Downregulated in CAC vs. CON (8 weeks)
506 DAVID IDs (Log2R<-1 & p<0.05)
enrichment score
extracellular matrix
secreted
collagen
VWFC
extracellular matrix structural constituent
laminin G domain
insulin-like growth factor binding
microtubule
EGF-like domain
Wnt signaling pathway
thrombospondin
immunoglobulin domain
leucine-rich repeat
fibronectin, type III
copper
actin-binding
L
weeks after tumor implantation
2 4 6 8
Acot1 mRNA levels (TPM)
Acot3 mRNA levels (TPM)
Apoe mRNA levels (TPM)
Cachectic
Control
Non-cachectic

Supplemental Figure S4, Related to Figure 4. The cachexia-inducing ("cachectic") melanoma tumors induce transcriptional changes in the liver, brown adipose, and white adipose tissue.

(A-D) Transcriptional changes induced in the liver. (A) Heatmap of 890 genes that are most highly modulated in the liver of cachectic mice, compared to controls. The average z-scores are color-coded (downregulated genes are shown in blue; upregulated genes are shown in red). (B) Upregulated genes include secreted proteins, protease inhibitors, lipocalins, and cell adhesion proteins. (C) Cachexia in the liver is characterized primarily by downregulation of gene expression, and categories such as "lipid metabolism", "endoplasmic reticulum", and "peroxisome" are over-represented. Genes modulated with $p<0.05$ and Log2R>1 (B) and Log2R<-1 (C) in the liver of cachectic melanomas versus control at 8 weeks post tumor implantation are shown. (D) Examples of genes downregulated by cachexia in the liver include regulators of lipid metabolism and peroxisomal proteins: *Fads2*, *Acsl1*, *Ecl1*, *Ddc*, *Pex6*, *Cat*, *Hadh*, and *Lpin2*.

(E-H) Transcriptional changes induced in the brown adipose tissue. (E) Heatmap of 1018 genes that are tightly associated with cachexia in the brown adipose tissue. The average z-scores are color-coded (downregulated genes are shown in blue; upregulated genes are shown in red). (F) Upregulated genes are the majority and include secreted proteins, complement pathway components, growth factors, and lysosomal proteins. (G) Few genes are downregulated by cachexia and these include secreted and transmembrane proteins. Genes modulated with $p<0.05$ and Log2R>1 (F) and Log2R<-1 (G) at 8 weeks post tumor implantation are shown. (H) Examples of genes upregulated by cachexia in the brown adipose tissue include lysosomal cathepsins *Ctsb* and *Ctsc*, and stearoyl-CoA desaturase-1 (*Scd1*).

(I-L) Transcriptional changes induced in the white adipose tissue. (I) Heatmap of 921 genes that are modulated by cachexia in the white adipose tissue. The average z-scores are color-coded (downregulated genes are shown in blue; upregulated genes are shown in red). (J) Upregulated genes include extracellular proteins, lipocalins, and regulators of lipid transport and metabolism. (K) Collagen, secreted proteins, and microtubule components are among downregulated genes. Genes modulated with $p<0.05$ and Log2R>1 (J) and Log2R<-1 (K) at 8 weeks post tumor implantation are shown. (L) Examples of genes upregulated by cachexia in the white adipose tissue include proteins involved in lipid metabolism: *Acot1*, *Acot3*, and *Apoe*.

In all graphs in (A-L), the bars represent SD, n is indicated; TPM indicates transcripts per million reads. All comparisons are significant ($p<0.05$) in cachectic versus control at 8 weeks post tumor cell injection.

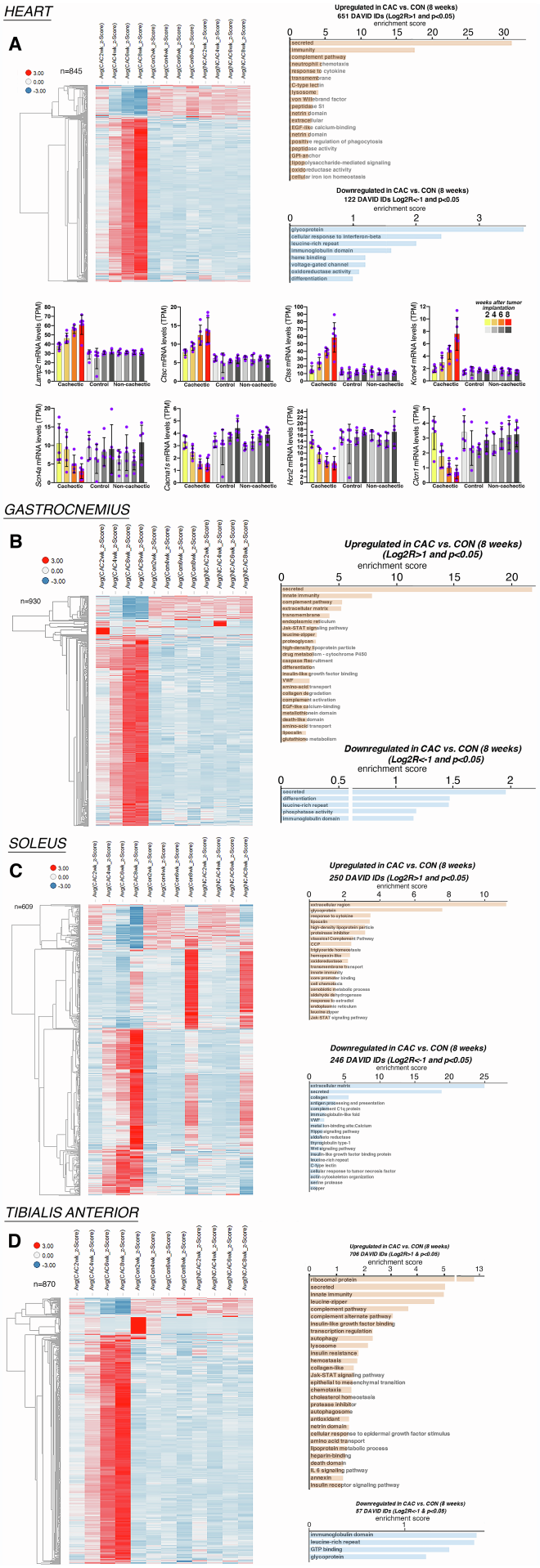
HEART
A
n=845
Upregulated in CAC vs. CON (8 weeks)
651 DAVID IDs (Log2R>1 and p<0.05)
enrichment score
secreted
immunity
complement pathway
neutrophil chemotaxis
response to cytokine
transmembrane
C-type lectin
lysosome
von Willebrand factor
peptidase S1
netrin domain
extracellular
EGF-like calcium-binding
netrin domain
positive regulation of phagocytosis
peptidase activity
GPI-anchor
lipopolysaccharide-mediated signaling
oxidoreductase activity
cellular iron ion homeostasis
Downregulated in CAC vs. CON (8 weeks)
122 DAVID IDs Log2R<-1 and p<0.05
enrichment score
glycoprotein
cellular response to interferon-beta
leucine-rich repeat
immunoglobulin domain
heme binding
voltage-gated channel
oxidoreductase activity
differentiation
weeks after tumor implantation
2 4 6 8
Lamp2 mRNA levels (TPM)
Cbx mRNA levels (TPM)
Ctss mRNA levels (TPM)
Kcnq4 mRNA levels (TPM)
Scn4a mRNA levels (TPM)
Cacna1s mRNA levels (TPM)
Hcn2 mRNA levels (TPM)
Clcn1 mRNA levels (TPM)
Cachectic
Control
Non-cachectic
GASTROCNEMIUS
B
n=930
Upregulated in CAC vs. CON (8 weeks)
(Log2R>1 and p<0.05)
enrichment score
secreted
innate immunity
complement pathway
extracellular matrix
transmembrane
endoplasmic reticulum
Jak-STAT signaling pathway
leucine-zipper
proteoglycan
high-density lipoprotein particle
drug metabolism - cytochrome P450
caspase Recruitment
differentiation
insulin-like growth factor binding
VWF
amino-acid transport
collagen degradation
complement activation
EGF-like calcium-binding
metallothionein domain
death-like domain
amino-acid transport
lipocalin
glutathione metabolism
Downregulated in CAC vs. CON (8 weeks)
(Log2R<-1 and p<0.05)
enrichment score
secreted
differentiation
leucine-rich repeat
phosphatase activity
immunoglobulin domain
SOLEUS
C
n=609
Upregulated in CAC vs. CON (8 weeks)
250 DAVID IDs (Log2R>1 and p<0.05)
enrichment score
extracellular region
glycoprotein
response to cytokine
lipocalin
high-density lipoprotein particle
protease inhibitor
classical Complement Pathway
CCP
triglyceride homeostasis
hemopexin-like
oxidoreductase
transmembrane transport
innate immunity
core promoter binding
cell chemotaxis
pancreatic metabolic process
aldehyde dehydrogenase
response to estradiol
endoplasmic reticulum
leucine-zipper
Jak-STAT signaling pathway
Downregulated in CAC vs. CON (8 weeks)
246 DAVID IDs (Log2R<-1 and p<0.05)
enrichment score
extracellular matrix
secreted
collagen
antigen processing and presentation
complement C1q protein
immunoglobulin-like fold
VWF
metal ion-binding site:Calcium
Hippo signaling pathway
aldo/keto reductase
thyroglobulin type-1
Wnt signaling pathway
insulin-like growth factor binding protein
leucine-rich repeat
cysteine rich
cellular response to tumor necrosis factor
actin cytoskeleton organization
serine protease
calpain
TIBIALIS ANTERIOR
D
n=870
Upregulated in CAC vs. CON (8 weeks)
706 DAVID IDs (Log2R>1 & p<0.05)
enrichment score
ribosomal protein
secreted
innate immunity
leucine-zipper
complement pathway
complement alternate pathway
insulin-like growth factor binding
transcription regulation
autophagy
lysosome
insulin resistance
hemostasis
collagen-like
Jak-STAT signaling pathway
epithelial to mesenchymal transition
chemotaxis
cholesterol homeostasis
protease inhibitor
autophagosome
antioxidant
netrin domain
cellular response to epidermal growth factor stimulus
amino acid transport
lipoprotein metabolic process
heparin-binding
death domain
IL6 signaling pathway
annexin
insulin receptor signaling pathway
Downregulated in CAC vs. CON (8 weeks)
57 DAVID IDs (Log2R<-1 & p<0.05)
enrichment score
immunoglobulin domain
leucine-rich repeat
GTP binding
glycoprotein

Supplemental Figure S5, Related to Figure 4. The cachexia-inducing ("cachectic") melanoma tumors induce transcriptional changes in the heart and skeletal muscles.

Transcriptional changes induced in the heart. (A) Heatmap of 845 genes that are most highly modulated in the heart of cachectic mice, compared to controls. The average z-scores are color-coded (downregulated genes are shown in blue; upregulated genes are shown in red). Most of these genes are upregulated whereas fewer are downregulated. Upregulated genes include secreted proteins, complement pathway components, and lysosomal and immune proteins. Downregulated genes are enriched for voltage-gated channels and glycoproteins. Genes modulated with $p<0.05$ and $Log2R>1$ and $Log2R<-1$ in the heart of cachectic melanomas versus control at 8 weeks post tumor implantation are shown. Examples of genes upregulated by cachexia in the heart include lysosomal proteins, such as *Lamp2*, *Ctsc*, and *Ctss*, which may drive heart wasting via the autophagy/lysosome system. Upregulation of *Kcne4* and downregulation of *Scn4a*, *Cacna1s*, *Hcn2*, and *Clcn1* ion channels also occurs in cachexia, and these changes in ion channel expression have been previously linked with arrhythmias and heart dysfunction. Bars represent SD, n is indicated; TPM indicates transcripts per million reads. All comparisons are significant ($p<0.05$) in cachectic versus control at 8 weeks post tumor cell injection.

Transcriptional changes induced in the gastrocnemius skeletal muscle. (B) Heatmap of 930 genes that are most highly modulated in the gastrocnemius muscle by cachectic melanoma xenografts compared to controls. These consist primarily of cachexia-upregulated genes that include secreted, Jak/Stat, endoplasmic reticulum, and other upregulated proteins ($p<0.05$ and $Log2R>1$). Downregulated proteins ($p<0.05$ and $Log2R<-1$) include secreted proteins and phosphatases.

Transcriptional changes induced in the soleus skeletal muscle. (C) Heatmap of 609 genes that define the impact of melanoma-induced cachexia on the soleus, compared to controls. Upregulated genes include extracellular proteins, complement pathway components, lipocalins, and genes involved in triglyceride homeostasis. Downregulated genes are enriched for secreted and extracellular matrix proteins.

Transcriptional changes induced in the tibialis anterior skeletal muscle. (D) Heatmap of 870 genes that define the impact of melanoma-induced cachexia on the tibialis anterior, compared to controls. Upregulated genes, which are the majority, include ribosomal and secreted proteins, complement pathway components, and autophagy/lysosome components. Downregulated genes are enriched for proteins with immunoglobulin domains. Genes modulated with $p<0.05$ and $Log2R>1$ and $Log2R<-1$ in tibialis anterior muscles of cachectic versus control mice at 8 weeks post tumor implantation are shown.

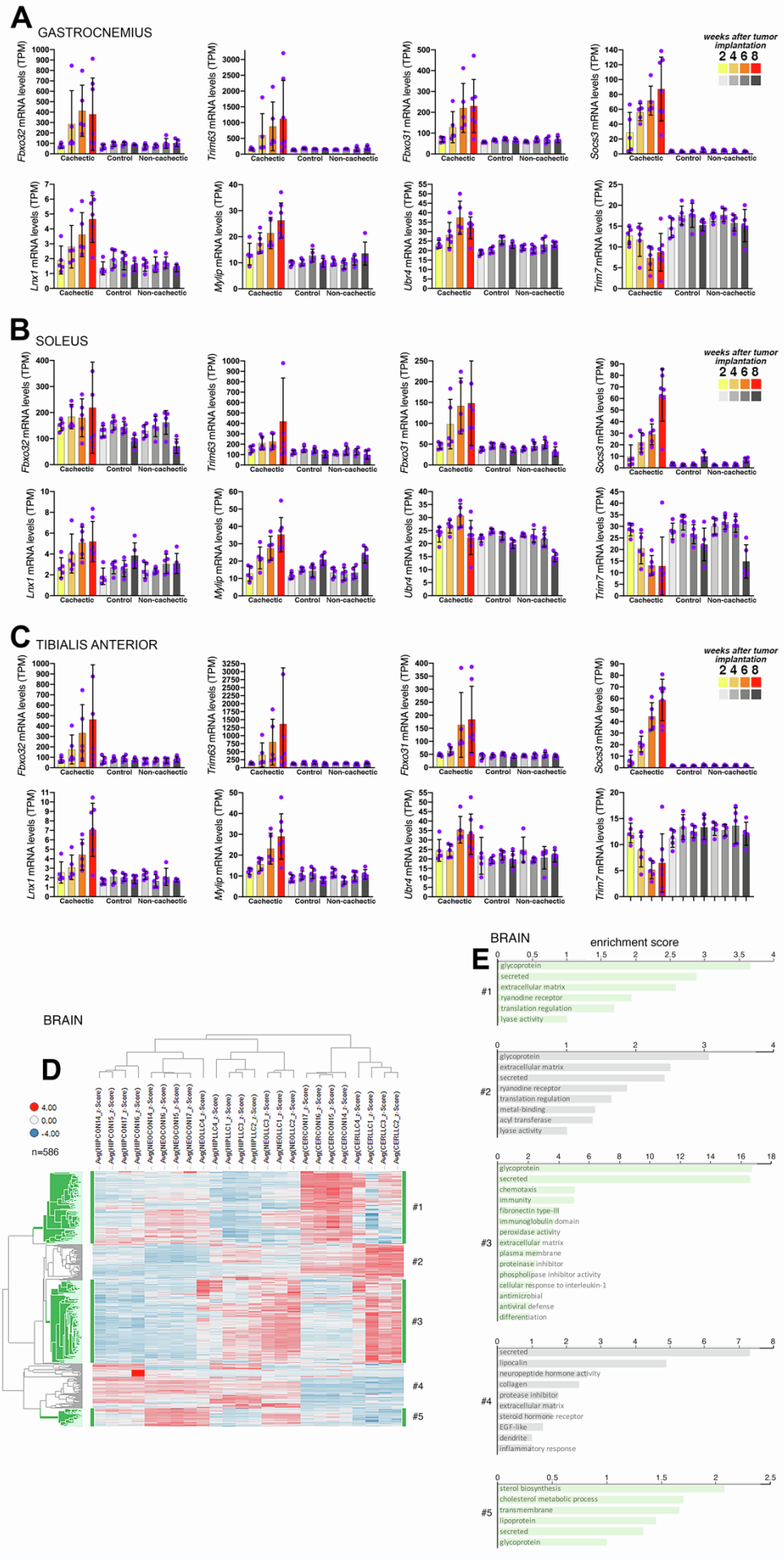
A
GASTROCNEMIUS
B
SOLEUS
C
TIBIALIS ANTERIOR
weeks after tumor implantation
2 4 6 8
Fbxo32 mRNA levels (TPM)
Trim63 mRNA levels (TPM)
Fbxo31 mRNA levels (TPM)
Socs3 mRNA levels (TPM)
Lnx1 mRNA levels (TPM)
Mylip mRNA levels (TPM)
Ubr4 mRNA levels (TPM)
Trim7 mRNA levels (TPM)
Cachectic
Control
Non-cachectic
D
BRAIN
4.00
0.00
-4.00
n=586
#1
#2
#3
#4
#5
E
BRAIN
enrichment score
#1
glycoprotein
secreted
extracellular matrix
ryanodine receptor
translation regulation
lyase activity
#2
glycoprotein
extracellular matrix
secreted
ryanodine receptor
translation regulation
metal-binding
acyl transferase
lyase activity
#3
glycoprotein
secreted
chemotaxis
immunity
fibronectin type-III
immunoglobulin domain
peroxidase activity
extracellular matrix
plasma membrane
proteinase inhibitor
phospholipase inhibitor activity
cellular response to interleukin-1
antimicrobial
antiviral defense
differentiation
#4
secreted
lipocalin
neuropeptide hormone activity
collagen
protease inhibitor
extracellular matrix
steroid hormone receptor
EGF-like
dendrite
inflammatory response
#5
sterol biosynthesis
cholesterol metabolic process
transmembrane
lipoprotein
secreted
glycoprotein

Supplemental Figure S6, Related to Figures 4 and 5. (A-C) Examples of E3 ubiquitin ligases modulated by melanoma-induced cachexia in skeletal muscles. Cachexia prominently induces E3 ubiquitin ligases already implicated in atrophy (*Fbxo32*, *Trim63*, *Fbxo31*, *Socs3*) as well as other E3s not previously associated with wasting (*Lnx1* and *Mylip*) in the gastrocnemius (A), soleus (B), and tibialis anterior (C) skeletal muscles. Ubr4 is significantly modulated in the tibialis anterior and gastrocnemius but not in the soleus muscle. While these E3s were upregulated in skeletal muscle by cachexia, other E3s such as *Trim7* are significantly downregulated. Unless otherwise noted, all comparisons are significant ($p<0.05$) in cachectic versus control at the 8 weeks post tumor cell injection. The graphs report the mean ±SD, the N is indicated. (D-E) The cachexia-non-inducing ("non-cachectic") melanoma tumors do not induce body and tissue wasting. (D) Heatmap of 586 genes (divided in 5 clusters) that are most highly modulated by LLC cancer cells in brain regions (cerebellum, hippocampus, neocortex) compared to controls. (E) Different gene categories are enriched in these 5 clusters, including secreted and extracellular proteins (clusters #1 and #2), proteins involved in immunity and chemotaxis (cluster #3), lipocalins and neuropeptides (cluster #4), and sterol biosynthesis (cluster #5).

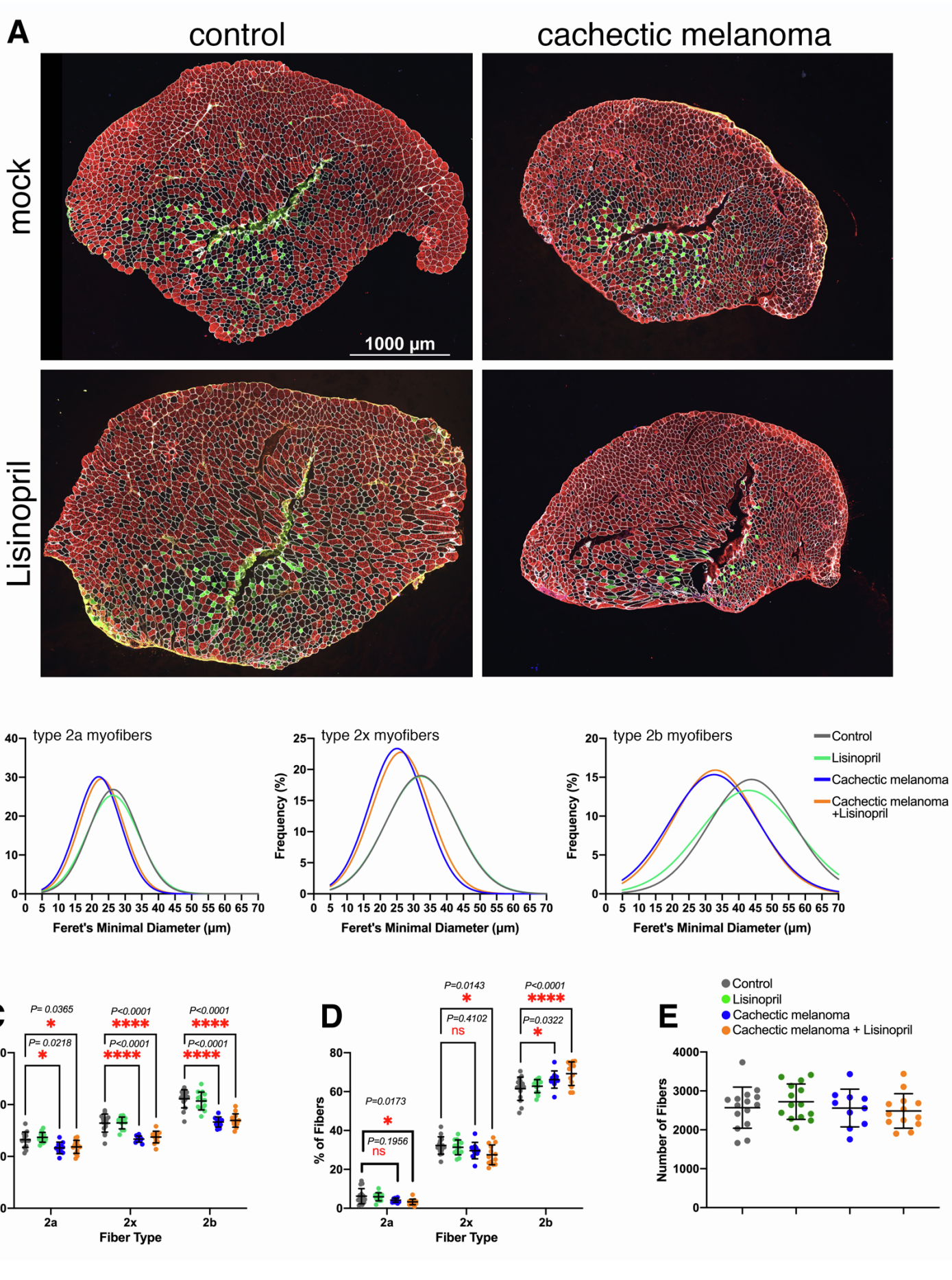
A
control
cachectic melanoma
mock
Lisinopril
1000 µm
B
type 2a myofibers
type 2x myofibers
type 2b myofibers
Frequency (%)
Feret's Minimal Diameter (µm)
Control
Lisinopril
Cachectic melanoma
Cachectic melanoma +Lisinopril
C
Feret's minimal diameter (µm)
P= 0.0365
P= 0.0218
P<0.0001
P<0.0001
P<0.0001
P<0.0001
2a
2x
2b
Fiber Type
D
% of Fibers
P=0.0173
P=0.1956
ns
P=0.0143
P=0.4102
ns
P<0.0001
P=0.0322
2a
2x
2b
Fiber Type
E
Control
Lisinopril
Cachectic melanoma
Cachectic melanoma + Lisinopril
Number of Fibers

Supplemental Figure S7, Related to Figure 7. Analysis of tibialis anterior muscles from mice implanted with cachectic melanomas and controls, and either treated with Lisinopril or mock-treated.
(A) Representative images of tibialis anterior (TA) muscle cross-sections from control mice and mice implanted with cachectic melanomas, and either mock-treated or treated with Lisinopril. (B) Frequency and gaussian distribution of Feret's minimal diameters for type 2a, 2x, and 2b myofibers from TA muscles sourced from control mice (gray), control mice treated with Lisinopril (green), mice implanted with cachectic melanoma xenografts (blue), and mice implanted with cachectic melanoma xenografts and treated with Lisinopril (orange). Melanoma xenografts reduce myofiber size but Lisinopril does not impact myofiber size. (C) Similar results are found with the analysis of the Feret's minimal diameter of different myofiber types from each TA muscle: there is significant decline in the size of type 2a, 2x, and 2b myofibers but this is not affected by Lisinopril. (D) Melanoma-induced cachexia tends to decrease the percentage of type 2a and type 2x myofibers and to correspondingly increase the percentage of type 2b myofibers. Whereas Lisinopril has no effect by itself, it significantly decreases the percentage of type 2a and 2x myofibers and increases the percentage of type 2b myofibers in conjunction with cachexia. (E) There are no significant changes in the total number of myofibers present in TA muscles in response to cachexia and/or Lisinopril treatment. In (C-E), the mean $\pm$SD is shown with *$p<0.05$ and ****$p<0.0001$ with n(TA)=15 for control mice, n(TA)=14 for control mice treated with Lisinopril, n(TA)=10 for mice implanted with cachectic melanomas and mock-treated, and n(TA)=13 for mice implanted with cachectic melanomas and treated with Lisinopril.